Lasers in Surgery and Medicine 28:313–319 (2001)

Optical-Thermal Simulation of Tonsillar Tissue Irradiation

Rahul K. Shah, MD,[1]* Babak Nemati, PhD,[2] Lihong V. Wang, PhD,[3] and Stanley M. Shapshay, MD[1]
[1]*Department of Otolaryngology-Head and Neck Surgery, Tufts-New England Medical Center, Boston, Massachusetts*
[2]*San Diego, California*
[3]*Optical Imaging Laboratory, Texas A&M University, College Station, Texas*

Background and Objective: Despite laser applications targetted toward tonsillar tissue, there has been no characterization of underlying optical and thermal events during laser irradiation of tonsillar tissue.
Study Design/Materials and Methods: The optical properties of canine and human tonsils were determined at 805 nm (diode laser) and 1,064 nm (Nd:YAG laser). An optical-thermal simulation was developed to predict the temperature rise in irradiated human tonsils.
Results: The optical properties of human and canine tonsillar tissue are similar at both wavelengths. The optical-thermal simulation was validated and predicts that at 10 W and 1 minute of irradiation, the heat will be contained within the human tonsil. The diode laser causes more superficial heating than the Nd:YAG laser.
Conclusions: The safety of irradiating human tonsils was shown. The diode laser is superior to the Nd:YAG laser because less heat affects collateral structures. The optical-thermal simulation detailed in this study can be used to predict the temperature rise in tissues undergoing irradiation. Lasers Surg. Med. 28:313–319, 2001.

Key words: laser-tissue interactions; mucosa intact laser tonsillar ablation; optical properties

INTRODUCTION

Tonsillectomies are one of the more commonly performed operations. Because of the vascular nature of the procedure, there is some morbidity and mortality associated with tonsillectomies [1]. The laser has been proposed as a surgical tool for tonsillectomies with the intent of reducing the morbidity and mortality of this operation. A myriad of laser systems have been proposed as alternatives to conventional tonsillectomities: CO_2 laser excision, interstitial photocoagulation, and mucosal intact ablation [1].

Despite various laser applications focusing on tonsillectomies, there has been no characterization of the underlying optical and thermal events during the laser irradiation of tonsillar tissue [2]. Fundamental quantities in laser-tissue interactions and the optical properties of a tissue have yet to be elucidated for tonsillar tissue. Laser-tissue interactions are often simulated by using transport models that rely on the measured optical and thermal properties of tissue. The optical properties of tissue consist of the scattering coefficient, $\mu_s[cm^{-1}]$, the absorption coefficient, $\mu_a[cm^{-1}]$, the refractive index, n, and the anisotropy factor, g [3]. The scattering coefficient is the inverse average distance a photon propagates before undergoing a scattering event [3]. Similarly, the absorption coefficient is the inverse average distance a photon will propagate in the medium before being absorbed [3]. The anisotropy factor, a measure quantifying the deflection angle caused by scattering, ranges between -1 and 1. A value of zero indicates isotropic scattering, a value of -1 indicates complete backward scattering, and a value of 1 is indicative of complete forward scattering [3].

Simulation models facilitate the evaluation of a wide range of parameters (e.g., deposited energy, wavelength, and duration of irradiation) for a desired outcome without the need for extensive in vivo trials. Once a desired outcome is approximated, the parameters can be further narrowed by a limited number of in vivo trials. Modeling applications result in a reduction of pre clinical animal experiments, previously necessary to find an optimum dosimetry, and facilitate further refinement of existing procedures leading to safer and more efficacious laser applications.

In this study, the optical properties of canine and human tonsillar tissue were determined by the adding-doubling method using a double-integrating sphere system [4–8] at wavelengths of 805 nm and 1,064 nm. The optical properties were used as inputs for an optical-thermal simulation program that was developed to predict the temperature rise in irradiated tissue. The validity of the model was corroborated by comparison with real-time temperature measurements obtained during irradiation of canine tonsillar tissue. The irradiation parameters used to predict the temperature rise during human tonsillar tissue irradiation were based on the Mucosal Intact Laser Tonsillar Ablation (MILTA) study [1]. In the MILTA study, investigators irradiated the surface of canine tonsils and subsequently showed tonsillar atrophy over the course of 45 days [1–9]. This technique has been proposed for irradiation of human tonsillar tissue, but the safety of the procedure needs to be further elucidated. Once validated, the optical-thermal simulation was then used to predict the response of human tonsillar tissue to the MILTA irradiation parameters.

*Correspondence to: Rahul K. Shah, 1530 Beacon Street, Apt. 707, Brookline, MA 02446. E-mail: banuandrahul@aol.com
Accepted 14 September 2000

MATERIALS AND METHODS

Determination of Optical Properties

The optical properties of human and canine tonsillar tissue were measured by using a double-integrating sphere system to obtain the reflectance and transmittance of the tissues [4–8], which are required inputs for the Inverse-Adding Doubling program [3]. The outputs of this program are the albedo (a), the optical thickness (τ) and anisotropy (g) of the tissue. With a tissue of known thickness (d), the absorption coefficient (μ_a) and scattering coefficient (μ_s) can be calculated from the following equation $\mu_a = (1 - a)\tau/d$ and $\mu_s = a\tau/d$ [6].

The integrating spheres are constructed from two stainless steel spheres (McMaster-Carr, New Brunswick, NJ), 5 inches in diameter, coated with barium sulfate paint (Kodak, Rochester, NY). Each sphere has three holes: an entrance (15 mm diameter) and exit (15 mm diameter) port for the beam, located directly opposite from one another and a port (9 mm diameter) for the photodetector [5]. A baffle was placed between the port abutting the sample in each sphere and the photodetector to ensure that no light reaches the detector directly from the sample.

The reflected and transmitted photons were measured with photodiodes (Hamamatsu, San Jose, CA). Four photodiodes were used: one as a reference, one in each the reflectance and transmittance spheres, and one for a collimated transmittance measurement. The reference detector was used to monitor the stability of the signal and all measurements were normalized by the intensity of this detector [7]. The photodiodes were connected to a transimpedance amplifier with a frequency bandwidth of 10 kHz. The amplified signal from each photodiode was then processed by a lock-in amplifier (Stanford Research Systems, Sunnyvale, CA). The lock-in amplifier used an optical chopper with a frequency of 400 Hz. The transimpedance amplifier and the lock-in amplifier were both used to increase the signal to noise ration of the detected signal. A neutral density filter was placed in front of the collimated transmittance detector to attenuate the light so to avoid detector saturation [7].

The reflectance and transmittance of the tonsillar tissue were measured from fresh tissue; the tissue was not preserved. The human tonsils were obtained, with approval of the New England Medical Center Research Committee, from patients undergoing a standard tonsillectomy procedure performed with electrocautery. The tonsillar tissue removed from these patients was immediately dissected, and the optical properties were measured. Canine tonsillar tissue was obtained from animals and used in other research protocols immediately after their killing. The tissue was prepared by cutting three to five serial sections from the body of each specimen (six specimens each from the human and canine). Each section was measured and then averaged with the other sections from that tonsillar tissue, and mean values for reflectance and transmittance for that tissue were obtained and subsequently averaged, with a mean for the human and canine tissue reported with a SEM. The section's tissue thickness measured an average of 1.0 mm. The sample was mounted between two glass slides and placed in a sample holder, positioned between the spheres. A thin layer of saline was applied between the slide and the tissue of prevent the formation of air bubbles [7]. The sample holder was positioned perpendicular to the incident beam. The percentage of light reflected and diffusely transmitted by the tissue was calculated by using a barium sulfate plate as a reference standard, and the reference photodiode to normalize the intensity of the measurements [7].

The wavelengths used to irradiate the tonsils for measurement of the reflectance and transmittance are 805 nm (Palomar, diode laser) and 1,064 nm (Zeiss, Nd:YAG laser). The light was delivered with a 600-μm fiber (Nd:YAG) and a 1,000-μm fiber (diode). The light from the lasers was attenuated with neutral density filters (Corion, Woburn, MA) placed at the output of the fiber. The light from the Nd:YAG laser was attenuated with 5% and 40% transmittance filters, and the light from the diode laser was attenuated with a 1% transmittance filter. The initial power was reduced to approximately 5 mW by the filters and a collimating iris, thus ensuring the tissue was not altered by the irradiation during the measurements [7].

The validity of the method was corroborated by determination of the absorption and scattering coefficients of tissues (liver and muscle) that were previously published [2].

In Vitro Temperature Measurements

Tonsils were removed from canines killed for other research purposes and the tissue was stored at 4°C in saline until laser irradiation was performed. The tonsils were placed in a container to stabilize the tissue and facilitate positioning of the 300-μm diameter thermocouple probes (type-T) in the tonsillar tissue. In an attempt to mimic in vivo conditions as closely as possible, beef was placed around the tonsillar tissue to create a pouch, similar to the pharyngeal cavity that surrounding the tonsil.

The container with the tonsil was submerged in a saline bath at 37°C until the surface of the tonsil was 2 mm below the saline. The thermocouples were positioned at depths of 2, 4, 6, 8, and 10 mm below the surface of the tonsil. The thermocouples were connected to an amplifier and a data acquisition system. The data were obtained via a computer data acquisition system and the software application LabView (National Instruments, Austin, TX).

The lasers used to irradiate the tonsils were the 1,064 nm Nd:YAG and 805 nm diode laser described above, with a spot size of 4 mm. The laser energy was delivered in a pseudo-pulsed mode so that the absorption of laser energy by the thermocouples could be identified [10]. The tissue was irradiated for 10 seconds, and then the laser was shut off for 1 second. The cooling of the thermocouple was shown to be much more rapid than the tissue cooling [10]. Thus, the thermocouple measurement at 11 seconds was the actual temperature of the tissue. Our studies confirmed that the psuedo-pulsed parameters used by others

[10] provided the highest duty cycle while providing adequate time for the thermocouple to cool.

The duration of irradiation, 1 minute, was based on the duration of irradiation during the MILTA procedure [1,9]. In the MILTA procedure, the laser fiber is moved across the length of the tonsil (average length of 20 mm) at a rate of 5 mm/10 s. Thus, over a 4-minute time period, a 5-mm longitudinal section of the tonsil is irradiated for about 60 seconds [1,9]. The most accurate irradiation time to mimic the MILTA dosimetry would be 1 minute.

Four pieces of tissue were used at each dosimetry, and the mean was obtained for a specific irradiation parameter, and the standard deviation of the mean was calculated.

Optical-Thermal Simulation

Simulation development. The optical simulation of light distribution during laser irradiation was based on a Monte Carlo model, as implemented previously for simple tissue geometry [11–17]. We used the delta-scattering technique [11] for photon tracing to greatly simplify the algorithm because this technique allows a photon packet to be traced without directly dealing with photon crossings of interfaces between different tissue types. This technique can be used only for refractive-index-matched tissues, although it allows the ambient clear media (e.g., air) and the tissue to have mismatched refractive indices. Because most soft tissues have similar indices of refraction, this limitation does not pose a problem in our simulation.

A Cartesian coordinate system was set up for the simulation. The origin of the coordinate system was the center of the incident optical beam on the surface of the turbid medium. The z axis was the normal of the surface pointing toward the inside of the turbid medium. The xy plane was therefore on the surface of the turbid medium.

We assumed that the tissue system had multiple tissue types with identical refractive indices. The interaction coefficient of the ith tissue type, defined as the sum of μ_a and μ_s, was denoted by μ_i. The delta-scattering technique applied to light transport in turbid media is briefly summarized as follows.

1. Define a majorant interaction coefficient μ_m, where $\mu_m \geq \mu_i$ for all i. In this study, μ_m was set to the maximum μ_i among all tissue types.
2. Select a step size R between two consecutive interactions based on the majorant interaction coefficient,

$$R = -\ln(\xi_R)/\mu_m, \tag{1}$$

where ξ_R was a uniformly distributed random number between 0 and 1 ($0 < \xi_R \leq 1$). Then, determine the tentative next collision site r'_k by

$$r'_k = r_{k-1} + Ru_{k-1}, \tag{2}$$

where r_{k-1} was the current site, and u_{k-1} was the direction of the flight. The direction of the flight was determined according to the probability distributions of deflection and azimuthal angles at each interaction site [15].
3. Play a rejection game:
   a. Get another random number ξ_a, which was uniformly distributed between 0 and 1 ($0 < \xi_a \leq 1$).
   b. If $\xi_a \leq \mu_i(r'_k)/\mu_m$, i.e., with a probability of $\mu_i(r'_k)/\mu_m$, accept this point as a real interaction site ($r_k = r'_k$).
   c. Otherwise, do not accept r'_k as a real interaction site, but select a new path starting from r'_k with the unchanged direction u_{k-1} (i.e., set $r_{k-1} = r'_k$ and return to step 2)

At each real interaction site, a fraction $\mu_a/(\mu_a + \mu_s)$ of the photon packet was absorbed, and the rest was scattered. The tracing continued until either the weight of the photon packet was below a preset threshold or the packet exited the tissue system. A subthreshold photon packet experienced a "Russian roulette" to conserve energy. Because step 3 was very efficient, the delta-scattering technique was comparable with the standard Monte Carlo simulation methods in computational speed. The detailed treatment of photon tracing after step 3 was similar to that in [15] and will not be repeated here.

The validity of step 3 can be easily understood by introducing an imaginary interaction event that changed neither the weight nor the direction of the photon. This definition implied that such imaginary interactions were not physically observable, i.e., they could be introduced with any interaction coefficient at any point. We assumed that the majorant interaction coefficient μ_m was a sum of the real μ_{re} and imaginary μ_{im} interaction coefficients, where the real interaction coefficient μ_{re} was $\mu_i(r'_k)$. In the procedure outlined above, a fraction of the interactions,

$$\mu_{re}/\mu_m = \mu_{im}/\mu_m \tag{3}$$

were imaginary interactions. From another point of view, it was easy to see that on the average, for every μ_m total interactions, there would be μ_{re} interactions accepted as real interactions. The mean free path for the majorant interactions in the delta-scattering method was $1/\mu_m$, and the mean free path for the real interactions in the direct method was $1/\mu_{re}$. Therefore, the photon would move to the correct interaction site using the delta-scattering technique as it would using the direct method because

$$\mu_m(1/\mu_m) = \mu_{re}(1/\mu_{re}), \tag{4}$$

where the left-hand side meant the average distance travelled by the photon packet with μ_m total steps or μ_{re} real interactions in the delta-scattering method, and the right-hand side meant the average distance travelled with μ_{re} real interactions in the direct method. During the tracing of each weighted photon [15], the light absorption, reflection, or transmission were correspondingly scored into different arrays according to the spatial positions of the photon. Multiple photons were traced to achieve an acceptable statistical variation.

The absorbed optical energy is converted into thermal energy. The following heat transfer equation is used to model the thermal energy propagation.

$$k\left(\frac{\partial^2 T}{\partial x^2} + \frac{\partial^2 T}{\partial y^2} + \frac{\partial^2 T}{\partial z^2}\right) + q''' = \rho C_p \frac{\partial T}{\partial t}. \tag{5}$$

TABLE 1. Optical Properties of Tonsillar Tissue

Tonsil source	Diode 805 nm			Nd:YAG 1064 nm		
	μ_a (cm^{-1})	μ_s (cm^{-1})	g	μ_a (cm^{-1})	μ_s (cm^{-1})	g
Canine	0.667 ± 0.01	71.1 ± 0.95	0.892 ± 0.006	0.461 ± 0.05	50.2 ± 0.81	0.898 ± 0.004
Human	0.562 ± 0.06	72.7 ± 1.7	0.894 ± 0.003	0.394 ± 0.10	52.0 ± 0.65	0.901 ± 0.005

where k is the thermal conductivity [W/(cm °C)], T is the local temperature [°C], x, y, z are the coordinate [cm], q' is the volumetric heat source [W/cm^3], ρC_p is the volumetric specific heat [J/(cm^3 °C], and t is time [s]. For the tissue interface with the ambient medium, a convective boundary is used as follows.

$$q = hA(T - T_c). \quad (6)$$

where h is the heat transfer coefficient [W/cm^2 °C], and A is the area of element [cm^2].

Input parameters to the model. The optical simulation was performed by using the measured optical properties of canine tonsillar tissue for the diode and Nd:YAG laser wavelengths (Table 1). The refractive index of the tissue was assumed to be 1.37, and the anisotropy factor was fixed at 0.9. Each simulation was conducted for 1,000,000 photons. The thermal simulation was performed by assuming a constant surface temperature of 37°C (normal body temperature), and a thermal transfer coefficient of 0.075 W/cm^2°C [18]. The thermal conductivity of tissue was assumed to be 0.003 W/cm°C [18], and the volumetric heat capacity was set at 3.7 J/cm^3°C [18].

RESULTS

The mean optical properties of human and canine tonsillar tissue for the diode and Nd:YAG wavelengths are presented in Table 1. The scattering coefficients and values for the anisotropy factor are not significantly different between human and canine tonsils. As expected with increasing wavelength, the scattering coefficient is decreased, as shown by the lower scattering coefficient for the Nd:YAG laser than for the diode laser. At both wavelengths, the absorption coefficient for the canine tonsil is smaller than the human tonsil. This may be attributable to the nature of the specimens. The human tonsils were obtained from patients who had a tonsillectomy for enlarged tonsils, whereas the canine tonsils were removed from canines with no pathologic enlargement of their tonsils. The subsequent enlargement of the tonsil and stretch of the mucosal surface may have resulted in the different absorption coefficients in the human tonsils. Table 2 contains the real-time in vitro temperature measurements during laser irradiation of canine tonsillar tissue at both wavelengths. These data were used to validate the predictions of the optical-thermal simulation.

The optical simulation of the laser-irradiated tonsillar tissue was used to arrive at the distribution of fluence and rate of heat generation within the tissue volume. Figure 1 illustrates the simulated depth-resolved rate of heat generation, directly under the beam, for canine tonsillar tissue for the diode and Nd:YAG laser wavelengths. Note that because of the higher obsorption for the diode laser wavelength, the rate of heat generation for this wavelength is higher through the first 3 mm into the tissue. Because the temperature measurements were conducted at multiple depths within the tissue, the thermal model was used to predict the time-resolved temperature generated by laser irradiation (diode and Nd:YAG) at various depths within the tissue volume. Figures 2 and 3 illustrate that, when the uncertainty in the simulated and measured temperatures are taken into account, there is acceptable agreement between the measured and simulated temperature response of canine tonsillar tissue to both irradiation wavelengths. This agreement between the theoretical results and the measured temperature values serves to validate the use of our optical-thermal simulation in predicting the underlying laser-tissue interactions involved in laser irradiation in laser irradiation of tonsillar tissue. Given this confirmation, the same model was used to predict the temperature response of human tonsillar tissue

TABLE 2. Temperature of In Vitro Canine Tonsillar Tissue Irradiated at 10 W for 1 min.

Depth of thermocouple (MM)	Diode (805 nm)		Nd:YAG (1064 nm)	
	Mean (C°)	SD (C°)	Mean (C°)	SD (C°)
2	65.35	6.81	76.51	6.73
4	53.68	4.37	58.20	2.90
6	44.78	2.40	48.13	2.03
8	39.71	1.32	41.17	1.87
10	37.77	1.12	37.28	1.45

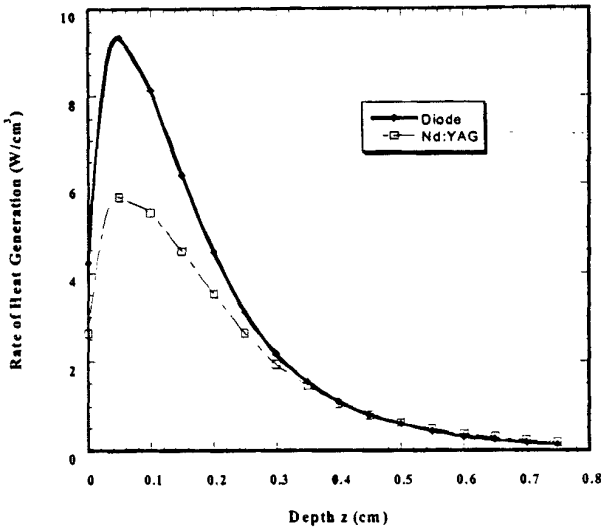

Fig. 1. Simulation of the depth resolved rate of heat generation (W/cm^3), directly under the beam, for tonsillar tissue irradiated by diode and Nd:YAG lasers.

to laser irradiation at both wavelengths. Figure 4 illustrates the simulated depth-resolved rate of heat generation within human tonsillar tissue that has been irradiated by diode and Nd:YAG lasers. Note that as in the case for canine tonsillar tissue, the rate of heat generation for the diode laser wavelength far exceeds that for the Nd:YAG

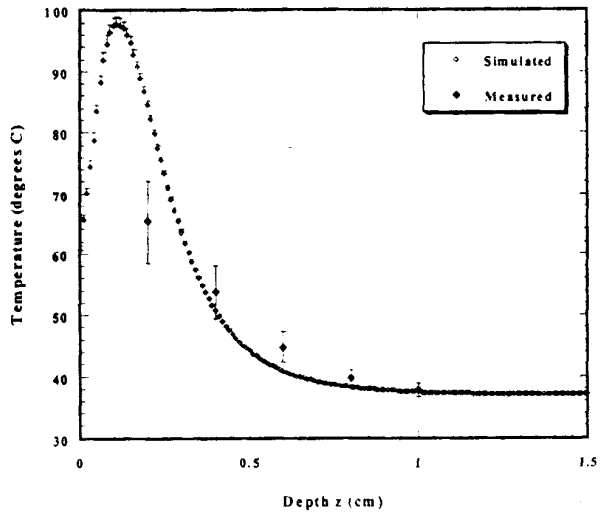

Fig. 2. Simulated and measured temperature response of canine tonsillar tissue to diode laser irradiation. The error bars shown for the "Simulated" data points are due to errors in the measurement of optical properties of tissue, and those for the "Measured" data points are due to variability in the in vitro temperature measurements. Temperature profile shown is for an irradiation time of 60 seconds.

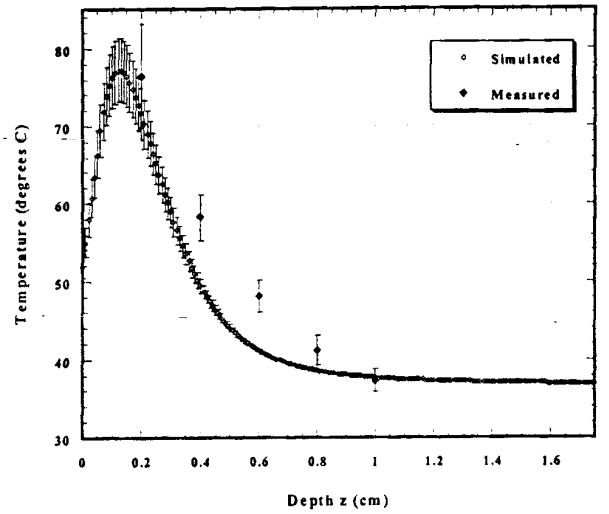

Fig. 3. Simulated and measured temperature response of canine tonsillar tissue to Nd:YAG laser irradiation. The error bars shown for the "Simulated" data points are due to errors in the measurement of optical properties of tissue, and those for the "Measured" data points are due variability in the in vitro temperature measurements. Temperature profile shown is for an irradiation time of 60 seconds.

laser wavelength for the first millimeter into the tissue. Figures 5 and 6 show a cross-sectional view of the simulated temperature profiles generated in human tonsillar tissue as a result of diode and Nd:YAG laser irradiation, respectively. These figures indicate that both wavelengths have comparable radial spread, even though the diode laser irradiation results in higher peak temperatures.

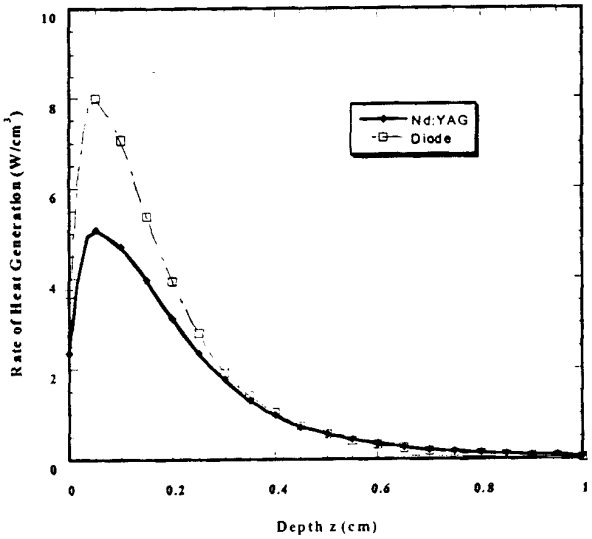

Fig. 4. Simulation of the depth resolved rate of heat generation (W/cm^3), directly under the beam, for human tonsillar tissue irradiated by diode and Nd:YAG lasers.

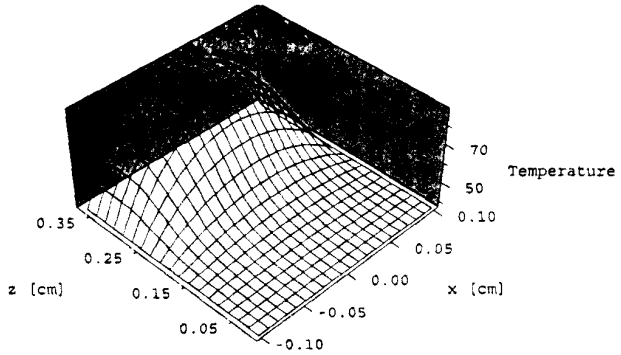

Fig. 5. Cross-sectional profile of the simulated temperature response of human tonsillar tissue to diode laser irradiation after 60 seconds of exposure.

DISCUSSION

The Mucosal Intact Laser Laser Tonsillar Ablation (MILTA) procedure was developed to reduce the blood loss and the time to recovery associated with conventional tonsillectomies. In the MILTA procedure, the oral cavity is filled with saline, and the tonsil (under this fluid layer) is irradiated in a noncontact mode for 4 minutes. After approximately 6 weeks, histopathology examination [1,9] has revealed complete absence of tonsillar tissue in the irradiated area. The advantages of this procedure are noteworthy: no bleeding, a rapid operation, and quicker recovery than a conventional tonsillectomy [1].

The pilot studies performed with the Nd:YAG laser were successful in showing the ablation of the tonsillar tissue [9]. The diode laser was proposed as an alternative to the Nd:YAG laser because the diode laser is a low-cost, portable, lightweight laser that offers the otolaryngologist the flexibility to use this surgical laser in the operating room or office settings [1]. In vivo canine studies with diode laser showed ablation of the tonsillar tissue with similar results as the Nd:YAG laser [1].

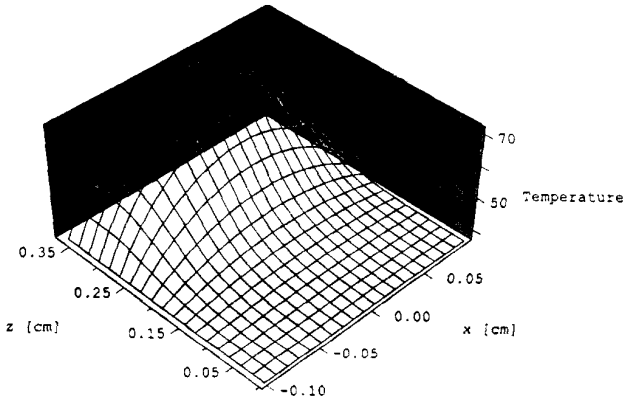

Fig. 6. Cross-sectional profile of the simulated temperature response of human tonsillar tissue to Nd:YAG laser irradiation after 60 seconds of exposure.

Despite the success of the MILTA procedure in in vivo canine studies, there have been concerns about the temperature elevation at the base of the tonsil [1]. Directly underneath the tonsil are important vascular structures that, if affected, could lead to hemorrhage or coagulative thrombi. The temperature measurements described in this study were performed to evaluate the temperature at the base of the tonsil during laser irradiation with the Nd:YAG and diode lasers. The in vitro conine tonsillar tissue results indicate that there is no significant difference in temperature rise at the base of the tonsil after laser irradiation at these two wavelengths (Table 2), suggesting that the heat is contained within the tonsillar tissue.

Although the safety of MILTA is clear in canine tonsils, establishing and safety of this technique in human tonsils is paramount. An optical-thermal simulation was developed to determine the response of human tonsillar tissue of the MILTA procedure. The optical properties (Table 1) show, a priori, the similarity between human and canine tonsillar tissue. The simulation results show that the laser energy is contained within the tonsil in both canine and human models (Figs. 5 and 6), even though there is a difference in the rate of heat generation in the superficial layers of these tissues when irradiated at the diode and Nd:YAG laser wavelengths (Fig. 4).

The simulation results support the use of the diode laser compared with the Nd:YAG laser because the thermal effect resulting from laser irradiation at the diode laser wavelength is concentrated superficially (Figs. 4–6). Because there will be variation among human tonsils, the laser with the least potential to cause temperature rises in the greater depth of the tonsil should be advocated. The diode laser is superior to the Nd:YAG laser for the MILTA procedure because of its more superficial effect that ensures minimal collateral thermal damage to surrounding tissues. In addition, the superficial thermal effect of diode laser irradiation would protect the underlying vasculature at the base of the tonsil from unwanted thermal damage.

Figures 5 and 6 also show minimal temperature rise in the mucosal surface of the tonsils at both wavelengths. This is consistent with the clinical results showing preservation of the mucosal surface and sheds insight into the pathophysiology of tonsillar atrophy in tonsils irradiated with the MILTA technique. Further studies investigating the novel mechanism of tonsillar ablation with noncontact laser irradiaton are currently being performed. The authors are also performing more modeling studies evaluating the optimum dosimetry for the MILTA procedure using the diode laser [19].

Measurement of the optical properties of human and canine tonsillar tissue and theoretical optical-thermal simulation of the underlying mechanisms involved in MILTA suggest the advantages of the diode laser over Nd:YAG laser irradiation for this procedure when applied to human tonsils. With diode laser irradiation, the heating is closer to the surface of the tonsil, resulting in less risk of heating the base of the tonsil. The optical similarity between human and canine tonsils supports extrapolation of irradiation parameters used in the in vivo canine study

[1,9] to the human patient with the expectation of being as safe and as efficacious as in the canine model. The optical thermal simulation presented in this article can also be used to rapidly evaluate laser irradiation parameters in various other laser applications.

REFERENCES

1. Volk MS, Wang Z, Pankratov MM, Perrault DF, Ingrams DR, Shapshay SM. Mucosa intact laser tonsillar ablation. Arch Otolaryngol Head Neck Surgery 1996;122:1355–1359.
2. Cheong WF, Prahl SA, Welch AJ. A review of the optical properties of biological tissues. IEEE J Quantum Electronics 1990;26:2166–2185.
3. Prahl SA. IAD Program Version 3.0, Downloaded from internet (www.ogi.edu), 1997.
4. Pickering JW, Moes CJM, Sterenborg HJCM, Prahl SA, van Gemert MJC. Two integrating spheres with an intervening scattering sample. J Opt Soc Am 1992;9:621–631.
5. Pickering JW, Prahl SA, van Wieringen N, Beek JF, Sterenborg HJCM, van Gemert MJC. Double-integrating-sphere system for measuring the optical properties of tissue. Appl Optic 1993;4:399–410.
6. Prahl SA, van Gemert MJC, Welch AJ. Determining the optical properties of turbid media by using the adding-doubling method. Appl Optics 1993;4:559–568.
7. Prahl SA. Optical Property Measurements Using the Inverse Adding Doubling Program, Oregon Medical Laser Center, Portland, Oregon; 1995.
8. Welch AJ, van Gemert MJC. Definition and Overview of Tissue Optics. Optical-Thermal Response of Laser-Irradiated Tissue. New York: Plenum Press;1995.
9. Wang Z, Pankratov MM, Volk MS, Perrault DF, Shapshay SM. 1.06-μm ND:YAG laser coagulation tonsillectomy: an animal study. Proc SPIE 1995;2395:354–359.
10. Anvari B, Motamedi M, Torres JH, Rastegar S, Orihuela E. Effects of surface irrigation on the thermal response of tissue during laser irradiation. Lasers Surg Med 1994;14:386–395.
11. Wilson BC, Adam GA. Monte Carlo model for the absorption and flux distributions of light in tissue. Med Phys 1983;10: 824–830.
12. Flock ST, Wilson BC, Wyman DR, Patterson MS. Monte-Carlo modeling of light-propagation in highly scattering tissues I: model predictions and comparison with diffusion-theory. IEEE Trans Biomed Eng 1989;36:1162–1168.
13. Prahl SA, Keijzer M, Jacques SL, Welch AJ. A Monte Carlo model of light propagation in tissue. In Muller GJ, Sliney DH, editors. Dosimetry of Laser Radiation in Medicine and Biology. Proc SPIE 1989;IS5:102–111.
14. Jacques SL, Wang LH. Monte Carlo modeling of light transport in tissues. In: Ashley J. Welch, Martin J.C. Van Gemert, Optical-Thermal Response of Laser-Irradiated Tissue (Laser, Photones, and Elector-Optics). New York: Plenum Press;1995.
15. Wang LH, Jacques SL, Zheng LQ. MCML—Monte Carlo modeling of photon transport in multi-layered tissues. Comput Methods Programs Biomed 1995;47:131–146. The MCML/CONV software package may be downloaded from URL:http://people.tamu.edu/~lwang.
16. Wang LH, Jacques SL, Zheng LQ. CONV—Convolution for responses to a finite diameter photon beam incident on multi-layered tissues. Comput Methods Programs Biomed 1997;54:141–150.
17. Lux I, Koblinger L. Monte Carlo Particle Transport Methods: Neutron and Photon Calculations. Boca Raton: CRC Press; 1991
18. Duck FA. Physical properties of Tissue: a Comprehensive Reference Book. New York: Academic Press;1990.
19. Shah RK, Nemati B, Wang LV, Volk MS, Shapshay SM. Optical-Thermal Simulation of Human Tonsillar Tissue Irradiation: Clinical Implications. Laser Surg Med 2000;27: 269–273.